American Journal of Pathology, Vol. 168, No. 1, January 2006

DOI: 10.2353/ajpath.2006.050342

*Molecular Pathogenesis of Genetic and Inherited Diseases*

# Defining a Link with Autosomal-Dominant Polycystic Kidney Disease in Mice with Congenitally Low Expression of *Pkd1*

Si-Tse Jiang,* Yuan-Yow Chiou,† Ellian Wang,* Hsiu-Kuan Lin,† Yuan-Ta Lin,* Ying-Chih Chi,* Chi-Kuang Leo Wang,* Ming-Jer Tang,‡ and Hung Li*§

*From the Institute of Molecular Biology,* Academia Sinica, Taipei; the Department of Pediatrics,† Institute of Clinical Medicine, National Cheng Kung University Medical Center, Tainan; the Department of Physiology,‡ National Cheng Kung University Medical College, Tainan; and the Institute of Biochemistry,§ National Yang-Ming University, Taipei, Taiwan*

**Mouse models for autosomal-dominant polycystic kidney disease (ADPKD), derived from homozygous targeted disruption of *Pkd1* gene, generally die *in utero* or perinatally because of systemic defects. We introduced a *loxP* site and a *loxP*-flanked *mc1-neo* cassette into introns 30 and 34, respectively, of the *Pkd1* locus to generate a conditional, targeted mutation. Significantly, before excision of the floxed exons and *mc1-neo* from the targeted locus by Cre recombinase, mice homozygous for the targeted allele appeared normal at birth but developed polycystic kidney disease with a slower progression than that of *Pkd*-null mice. Further, the homozygotes continued to produce low levels of full-length *Pkd1*-encoded protein, suggesting that slight *Pkd1* expression is sufficient for renal cyst formation in ADPKD. In this viable model, up-regulation of heparin-binding epidermal growth factor-like growth factor accompanied increased epidermal growth factor receptor signaling, which may be involved in abnormal proliferation of the cyst-lining epithelia. Increased apoptosis in cyst epithelia was only observed in the later period that correlated with the cyst regression. Abnormalities in $Na^+/K^+$-ATPase, aquaporin-2, and vasopressin V2 receptor expression were also identified. This mouse model may be suitable for further studies of progression and therapeutic interventions of ADPKD.** ***(Am J Pathol 2006, 168:205–220; DOI: 10.2353/ajpath.2006.050342)***

Autosomal-dominant polycystic kidney disease (ADPKD) is one of the most common life-threatening inherited diseases, characterized by the development of gradually enlarging renal cysts and a progressive loss of normal kidney tissue that can lead to chronic renal failure. It affects between 1 in 600 and 1 in 1000 live births in all ethnic groups worldwide. Cysts in the liver, pancreas, and spleen as well as a variety of cardiovascular, cerebrovascular, and connective tissue abnormalities are also common.[1] The fluid-filled cysts in an affected kidney are lined by monolayer epithelial cells derived from every segment of the nephron, but predominantly from the collecting duct.[2] The pathogenesis of the renal cyst formation and progression is currently thought to involve 1) dysregulated epithelial cell proliferation and differentiation, 2) alternations in specific membrane protein polarity, 3) changes in cell-matrix interactions, and 4) abnormality in fluid accumulation.[3] Since there is currently no effective treatment for ADPKD except for dialysis and renal transplantation, much attention has been focused on understanding the molecular mechanism underlying the pathogenesis of renal cyst expansion.

Throughout the past decade, the mutated genes responsible for ADPKD were identified by positional cloning strategies. In most cases, ADPKD is recognized as a monogenic disorder caused by mutation in two genes: *PKD1*, accounting for ~85% of cases; and *PKD2*, accounting for ~10% of cases.[4–7] Most mutations identified in affected families appear to inactivate the *PKD* genes. However, patients with ADPKD are heterozygotes, having inherited one mutant and one normal allele of the *PKD1* or *PKD2* genes. Studies of cyst-lining epithelial cells isolated from individual cysts in both disorders have demonstrated loss of heterozygosity at the wild-type *PKD1* allele[8,9] that has led to a two-hit mechanism for cyst

Supported by The National Research Program for Genomic Medicine (grant AS92IMB3) and the National Health Research Institute (postdoctoral fellowship award RE91N004 to S.-T.J.).

Accepted for publication September 19, 2005.

Address reprint requests to Hung Li, Ph.D., Institute of Molecular Biology, Academia Sinica, Nankang, Taipei 11529, Taiwan. E-mail: hungli@ccvax.sinica.edu.tw.

formation. This mechanism requires not only a germ-line mutation of *PKD1* or *PKD2* but also an additional somatic mutation in the wild-type gene to initiate the formation of cysts. Briefly, loss-of-function mutations in both alleles of either *PKD1* or *PKD2* are necessary and sufficient for renal cyst formation in ADPKD. The results of animal studies also support the two-hit mechanism because mice heterozygous for targeted disruption of either *Pkd1* or *Pkd2* develop late-onset renal cysts, whereas homozygous animals die *in utero* or perinatally with severe cystic disease.[10–12] This mechanism would explain the late age of onset in ADPKD and the focal nature of epithelial cells giving rise to cysts. Although such second hits do indeed occur within individual cysts, the frequencies are low (between 17% and 24% in *PKD1*).[8,13] In addition, the germ line wild-type *PKD1* is still expressed continuously in most cyst epithelial cells of kidneys from ADPKD patients having inherited one mutant *PKD1* allele.[14] The evidence suggests that the majority of somatic mutations in *PKD1* are likely to be missense changes if the two-hit mechanism is operational. In the present study, we found that only partial inhibition of *Pkd1* expression was sufficient for renal cyst formation in mice, suggesting the other possible mechanism that any actions hampering the expression and/or biological function of *PKD1* may initiate the renal cyst formation in ADPKD. Complete loss-of-function in either *PKD1* or *PKD2* may not be strictly required for development of the common ADPKD.

Polycystin-1, the novel protein encoded by *PKD1*, is a large (>460 kd) membrane protein of ~4300 amino acids with 11 transmembrane domains. Its extensive extracellular amino terminus contains a number of adhesive domains that implicate polycystin-1 in cell-cell and cell-matrix interactions.[3,5,6] The short intracellular carboxyl terminus of the protein has a G protein binding site and many sites for phosphorylation that could respond to regulators of signal transduction, as well as a coiled-coil domain that is in physical interaction with *PKD2*-encoded polycystin-2.[3,15] Polycystin-2 is also a membrane protein, with six transmembrane domains, that functions as a $Ca^{2+}$-permeant cation channel and has significant homology with the transient receptor potential family (TRP).[16] Recent studies have shown that polycystin-1 and polycystin-2 are interacting partners within a receptor-ion channel complex in which polycystin-1 acts as a receptor that gates $Ca^{2+}$-permeant polycystin-2 channels.[16] This polycystin complex has been found in primary cilia and basolateral membrane of renal epithelial cells, where it may participate in sensing fluid shear stress and cell-cell/matrix interaction, respectively.[17,18] However, the diverse functions of the polycystin complex are not fully characterized, and its roles in the process of renal cystic transformation are still under extensive investigation.

Polycystin-1 and -2 are widely expressed in fetal and adult tissues,[7,19] and their expressions are developmentally regulated.[20,21] Homozygous mutant mice with targeted disruption of either *Pkd* gene generally die *in utero* or perinatally with cardiac septal defects, bone abnormalities, and severe cystic manifestations in nephrons and pancreatic ducts.[10,11,22] These previous studies confirm the requirement of either *Pkd* gene during embryonic development.

Animal models are important tools in experimental medical science to understand better the pathogenesis of human diseases and to test therapeutic approaches. Currently, no mouse model for the most common and severe form of ADPKD derived from targeted disruption of *Pkd1* is viable and amenable for further investigation. In the experiments described herein, we used homologous recombination to introduce a Neo cassette into intron 34 of mouse *Pkd1* to partially inhibit its expression. The mouse homozygotes appear normal at birth but still have small renal cysts. Cyst enlargement and interstitial fibrosis are developed later, recapitulating the phenomena in the human ADPKD. The resulting mouse models for ADPKD are viable and suitable for advanced studies in the future.

## Materials and Methods

### Generation of Pkd1 Gene Targeting Mutant Mice and Breeding Scheme

A targeting plasmid was constructed using genomic DNA fragments derived from 129/Ola mouse strain. A loxP site, which has a neomycin cassette flanked by two loxP sites, and a thymidine kinase cassette were introduced into the *Pkd1* locus (Figure 1A). Embryonic stem (ES) cell (line E14) electroporation, selection, and screening were performed using standard gene targeting techniques. Briefly, genomic DNA was isolated from neomycin and gancyclovir double-resistant ES cell clones and screened for a specific targeting event by polymerase chain reaction (PCR) using a forward primer outside the targeting vector and downstream of exon 36 (5′-CAAAGCCCTGACTATCCATTGG-3′) and a reverse primer in the *neo* sequence (5′-CCTCTTGAAA-ACCACACTGCTCG-3′). The correct targeting of PCR-positive clones was confirmed by Southern blot analysis. For this analysis, 10 $\mu$g of DNA from selected clones was digested with *Xba*I, and DNA was electrophoresed and transferred onto nylon membranes using capillary transfer. Blots were hybridized with P32-labeled probe external to the targeting vector (Figure 1A). Blots were also hybridized with neo-specific probes to verify the absence of additional random integration of the targeting vector. To demonstrate the presence of the *loxP* in intron 30, one set of primers located upstream from the *loxP* site (5′-GGTAGGTCCTGTGAGGTTTGCTG-3′) and *neo* (5′-GC-CTTCTATCGCCTTCTTGACG-3′) were used. All of the PCR products amplified from positive clones were confirmed by sequencing. Positive clones were injected into C57BL/6 blastocysts to generate chimeras. The chimeras that were derived from C57BL/6 blastocysts were bred with C57BL/6 or FVB inbred strain mice. Homozygotes were generated by a cross between F1 heterozygotes, and heterozygotes and homozygotes were determined by Southern blot or PCR of tail genomic DNA.

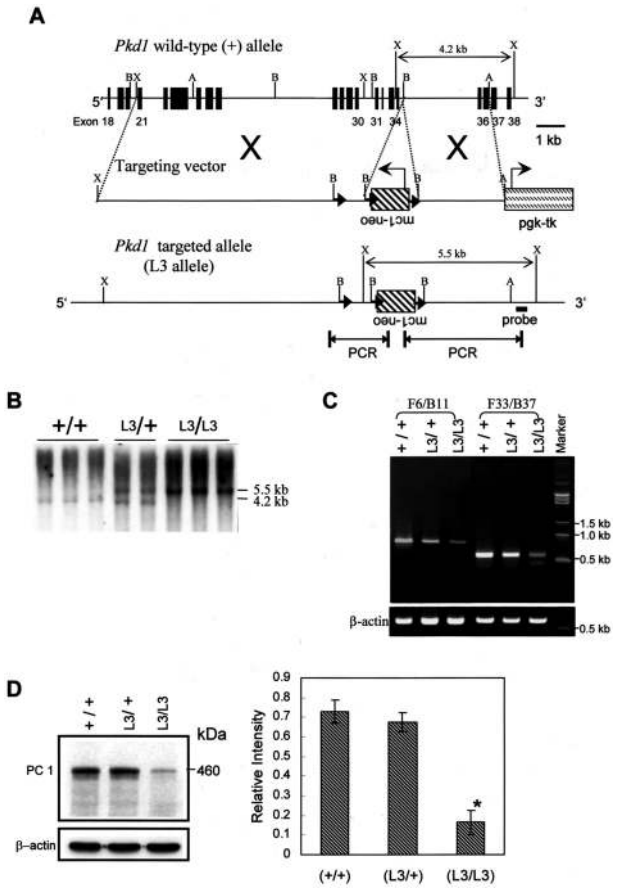


**Figure 1.** Targeting of the *Pkd1* locus by homologous recombination and expression of *Pkd1* in targeted mutants. **A:** Structure of wild-type and targeted *Pkd1* L3 alleles. The exons are numbered and depicted by **filled boxes**: B, *Bam*HI; X, *Xba*I; A, *Afl*II. An inverted mc1 promoter-driven neomycin resistance gene (mc1-neo), flanked by two *loxP* sites (**filled triangles**), was inserted into intron 34 of *Pkd1*. The third *loxP* site was inserted into intron 30 of *Pkd1*. A phosphoglycerate kinase (pgk) promoter-driven thymidine kinase gene (tk) was used for negative selection. Single **arrows** indicate the direction of transcription. Diagnostic restriction enzymes, probe for Southern blotting, and primers for PCR analysis are indicated. **B:** Southern blot analysis of targeted mouse mutants. DNA isolated from F2 littermates derived from intercrossing of F1 heterozygotes was digested with *Xba*I and hybridized with the probe outside the targeting vector. The 4.2- and 5.5-kb bands correspond to wild-type and mutant alleles, respectively. **C:** RT-PCR of *Pkd1* transcripts in the wild-type (+/+), heterozygous (L3/+), and homozygous (L3/L3) kidneys using primer sets F6/B11 and F33/B37 (see Experimental Procedures for primer information). Amplification of β-actin shows the equivalence of the RNA loading and amplification. **D:** Western blot analysis of membrane fraction from kidneys. Polyclonal antibodies against a peptide corresponding to amino acids 866 to 882 of murine polycystin-1 (PC1) detect a prominent ~460-kd band in wild-type (+/+) and heterozygote (L3/+) and is faint in the homozygote (L3/L3) mutants. β-Actin was used as a control for equal loading of protein. The intensity of the ~460-kd band relative to β-actin is shown in a chart on the **right**. The number of mice analyzed was $n = 6$ for each genotype. $^*P < 0.01$ compared with wild-type or heterozygous mice, using Kruskal-Wallis test. All results are representative of at least three mice per genotype in two independent experiments.

## *Reverse Transcriptase (RT)-PCR Analysis*

RT-PCR analysis was performed with 4 μg of total RNA extracted from various organs. First-strand cDNA was synthesized by Super Script II RT (Gibco BRL, Eggenstein, Germany) with 25 ng of oligo(dT)$_{12\text{-}18}$ primer and 200 U of Super Script II per reaction. Samples (5 μl) of the RT reaction were used in a 100-μl PCR reaction. Two sets of primers were used for analysis of the *Pkd1* transcript. Set 1, F6 in exon 6 (5′-AAGCACAGGAGCAATGTCGGAC-3′) and B11 in exon 11 (AATGAGGTCACCAGGGAGCATAGG-3′) amplified an 839-bp fragment from the wild-type *Pkd1* transcript. Set 2, F33 in exon 33 (5′-GGAAGATGGTGCCTCTCTGGTTAG-3′) and B37 in exon 37 (5′-CACACGCTCACTTACAGGGGTTAC-3′) amplified a 583-bp fragment from the wild-type *Pkd1* transcript. A set of primers was used for analysis of the EGF transcript; 5′-TCCGTCCGTCTTATCAGGCATC-3′ and 5′-GGCACATTCATTGACATCTTCGC-3′ amplified a 375-bp fragment. Another set of primers was used for analysis of the heparin-binding epidermal growth factor (HB-EGF) transcript; 5′-AAGTTGCTTTCTCCTCCAAGCC-3′ and 5′-CCACGATGACAAGAAGACAGACG-3′ amplified a 321-bp fragment. Each transcript from various genotyped mice was cloned and sequenced by the dideoxy method.

## *Antibodies*

We generated rabbit polyclonal antibodies specific for mouse polycystin-1 using a segment of the first extracellular PKD domain polypeptide (containing amino acids 866 to 882 of murine polycystin-1), as described in a previous study.[18] The peptide was also conjugated to NHS-activated Sepharose 4B (Amersham Biosciences, Uppsala, Sweden) for affinity purification of these polyclonal antibodies. A rabbit antiserum to Tamm-Horsfall glycoprotein was purchased from Biomedical Technologies Inc. (Stoughton, MA). A purified rabbit antibody to lysozyme was purchased from DakoCytomation (Glostrup, Denmark). Mouse monoclonal antibodies against erb-B2, $Na^+/K^+$-ATPase α1-chain, and proliferating cell nuclear antigen were purchased from Upstate Biotechnology (Lake Placid, NY). Mouse monoclonal antibodies against α-smooth muscle actin (α-SMA), $Na^+/K^+$-ATPase β2-chain, β-actin, Grb2, and Shc were purchased from BD Biosciences (Franklin Lakes, NY). Affinity-purified rabbit antibodies against EGF receptor and phospho-EGF receptor were purchased from Cell Signaling Technology (Beverly, MA). Affinity-purified goat polyclonal antibodies to aquaporin-2 were purchased from Santa Cruz Biotechnology Inc. (Santa Cruz, CA). A rabbit antiserum to $Na^+/K^+$-ATPase β1-chain was purchased from United States Biological (Swampscott, MA).

## *Western Blot Analysis*

For Western blot analysis, total protein was measured by Bio-Rad protein assay (Hercules, CA), for which 50 μg/lane of membrane and cytosol fractions from various tissue extracts were separated on sodium dodecyl sulfate-polyacrylamide gels at 80 V at room temperature. Protein was transferred onto polyvinylidene difluoride membrane at 35 V for 16 hours at 4°C in Tris-glycine transfer buffer. The membrane was blocked with 5% nonfat dry milk in Tris-buffered saline containing 0.1% Tween-20 and incubated with primary antibodies. The immunoreactive protein was captured by horseradish

peroxidase-conjugated secondary antibodies and was detected by enhanced chemiluminescence.

### Histology and Immunohistochemistry Studies

For histological analysis, specimens were fixed in formalin, embedded in paraffin, sectioned at 4 $\mu$m, and stained with hematoxylin and eosin (H&E) as well as Masson's trichrome for light microscopic examination. For immunostaining, a standard immunoperoxidase protocol (Vectastain ABC kit; Vector Laboratories, Burlingame, CA) was used. After blocking with goat serum, sections were incubated with primary antibodies for 1 hour at room temperature, rinsed in phosphate-buffered saline, incubated with biotinylated goat anti-rabbit or anti-mouse secondary antibodies, rinsed, then incubated with streptavidin-conjugated peroxidase, rinsed, then incubated with 3-amino-9-ethyl-carbazole or diaminobenzidine as a chromogen, counterstained with hematoxylin, and examined by light microscopy. For specific labeling of the collecting duct, sections were directly incubated with biotinylated *Dolichos biflorus* lectin (purchased from Vector Laboratories), rinsed, and then incubated with streptavidin-conjugated peroxidase. For morphometric analysis of the interstitial fibrosis in the kidney, a standard point-counting method was used to quantitate the matrix score for $\alpha$-SMA expression in the renal interstitium. Briefly, under high magnification ($\times$200), 12 nonoverlapping fields from each renal section were immunostained with $\alpha$-SMA and photographed. A grid containing 100 ($10 \times 10$) sampling points was superimposed on each photograph. Points falling on cystic cavities, glomerular structures, or large vessels were excluded from the total count. The staining scores of interstitial $\alpha$-SMA expression were assessed by the number of points overlying positive $\alpha$-SMA expression and then converted to a percentage.

### Apoptotic Index: Terminal dUTP Nick-End Labeling (TUNEL) Assay

For each genotype, 4-$\mu$m-thick sections of formalin-fixed renal tissue from 3-month-old mice were deparaffinized and hydrated in graded alcohols. After digestion in proteinase K and immersion in 2% $H_2O_2$, sections were incubated with 10 $\mu$mol/L biotin-16-dUTP and 0.2 U/$\mu$l TdT in TdT buffer [30 mmol/L Tris-HCl (pH 7.2), 140 mmol/L sodium cacodylate, 1 mmol/L cobalt chloride]. The enzymatic reaction was stopped by immersion in TB buffer (300 mmol/L sodium chloride, 30 mmol/L sodium citrate). After incubation with 2% bovine serum albumin, labeled nucleotides were reacted with avidin/biotin complex (Vectastain; Vector Elite, Burlingame, CA), followed by visualization with 3,3′-diaminobenzidine and counterstained with periodic acid-Schiff. Apoptosis was quantitated by averaging the number of stained nuclei per cystic and noncystic tubule in a minimum of 500 tubular epithelial cells/kidney.

## Results

### Generation of a Floxed Allele of Pkd1 for Cre-Mediated Conditional Knockout in the Mouse

Consistent with the broad expression of *Pkd1* during early organogenesis, mice homozygous for targeted disruption of *Pkd1* exhibit developmental abnormalities causing embryonic or perinatal lethality.[10,11,22,23] The complex renal and extra-renal phenotypes of the *Pkd1*-targeted mutants obstruct further investigation at later stages of development and mask direct from indirect consequences of *Pkd1* inactivation. To circumvent this limitation, we first created a floxed *Pkd1* mouse for conditional inactivation of polycystin-1 by Cre/*loxP*-mediated gene targeting. The targeted strategy and genotype analysis of the ES clones and mice are summarized in Figure 1, A and B. A single *loxP* site was inserted into intron 30, and a *loxP*-flanked mc1-neomycine (mc1-neo) cassette was inserted into intron 34 in reverse orientation relative to the targeted *Pkd1* gene. The linearized targeting vector was introduced into E14 ES cells by electroporation, and 279 colonies resistant to G418 and gancyclovir were selected. Sequencing of PCR products formed by primers outside the 3′ end of the short homologous arm and in the *neo* gene identified 21 independent ES cell clones with *Pkd1* targeted by homologous recombination. All these positive clones were double-checked by Southern blot analysis with a 3′-external probe. The presence of the *loxP* site in intron 30 of the targeted allele was confirmed in 15 clones by sequencing of the PCR products formed by primers 5′ upstream from the *loxP* site and in the *neo* gene. The remaining six clones contained only the *loxP*-flanked *mc1-neo* cassette in intron 34 of the targeted *Pkd1* allele (Lneo). Two independent clones (no. 175 and no. 186) with the *neo* gene and all three *loxP* sites in the targeted allele (L3) were injected into C57BL/6 blastocysts and implanted into pseudopregnant females. The resulting chimeric mice, with >80% of the agouti coat, were crossed with C57BL/6 or FVB mice to produce $Pkd1^{L3/+}$ F1 progeny. The phenotypes described below were not significantly influenced by genetic background. Most of the phenotypic analyses were performed with C57BL/6–129 background.

### Characterization of $Pkd1^{L3/L3}$ Mice

$Pkd1^{L3/+}$ F1 progeny derived from clone no. 175 were intercrossed and the F2 progeny were genotyped at 3 weeks of age (Figure 1B): 58 wild-type ($Pkd1^{+/+}$), 114 $Pkd1^{L3/+}$, and 54 $Pkd1^{L3/L3}$ animals are shown. Genotyping of the clone no. 186 F2 progeny showed 11 $Pkd1^{+/+}$, 25 $Pkd1^{L3/+}$, and 13 $Pkd1^{L3/L3}$ animals, similar to clone no. 175 F2 progeny. The ratio of $Pkd1^{+/+}$:$Pkd1^{L3/+}$:$Pkd1^{L3/L3}$ in either of the mouse lines did not differ significantly from the 1:2:1 ratio expected for a nonlethal mutation. Most of the phenotypic analyses were performed with the no. 175-derived mouse line, but identical results also were obtained with the no. 186-derived line. RT-PCR of total RNA from 30-day-old $Pkd1^{+/+}$, $Pkd1^{L3/+}$,

and *Pkd1*$^{L3/L3}$ mice, using 5′-exon 33 primer (F33) and 3′-exon 37 primer (B37), revealed only a single DNA band of predicted size for wild-type transcript in mRNA from all three genotyped mice (Figure 1C). DNA sequences of these RT-PCR products were identical, suggesting that the *mc1-neo* cassette in reverse orientation within intron 34 is not spliced into the *Pkd1* transcript of the *Pkd1* L3 allele. Interestingly, the transcript was expressed at a lower level in homozygotes after normalization with $\beta$-actin expression. RT-PCR analysis using the other set of primers located in exons 6 (F6) and 11 (B11) also showed a similar result (Figure 1C). To determine whether the protein level of polycystin-1 was also decreased in homozygous mutants, we performed Western blot analysis with a polyclonal antibody directed against the extracellular first PKD domain of mouse polycystin-1. A strong immunoreactive band of ~460 kd was detected in wild-type and heterozygous mice, and once again the intensity of this band showed a fourfold to fivefold decrease in homozygous mutants (Figure 1D). These results indicate that the insertion of the *mc1-neo* into intron 34 causes a significant disturbance but does not completely abrogate in *Pkd1* expression.

## *Development and Progression of Kidney Cystic Disease in Pkd1*$^{L3/L3}$ *Mice*

Unlike the previously established homozygous mutants with targeted disruption of *Pkd1*, the *Pkd1*$^{L3/L3}$ mice expressing a low level of polycystin-1 appeared normal at birth with no gross anatomical abnormality (Figure 2A). The short stature, distended abdomens, and massively enlarged cystic kidney were not exhibited until several days after birth (Figure 2). A total of 104 *Pkd1*$^{L3/L3}$ and 46 *Pkd1*$^{L3/+}$ mice (age range, 1 to 360 days) were examined for kidney size and cystic lesions in their pancreas and liver, as well as the size of their heart and lungs. Grossly, the kidneys of the *Pkd1*$^{L3/L3}$ mice enlarged rapidly during the first 30 days and gradually shrunk in volume by more than 50% thereafter, resulting in a bumpy and distorted appearance (Figure 2, E–H). We also successively measured the abdominal girth, an indirect indicator of kidney size, of the *Pkd1*$^{L3/L3}$ mice for 6 months. Coinciding with the finding of kidney size variations, the abdominal girths also rapidly increased during the first 30 days after birth and subsequently decreased. The massive translucent cysts in bilateral kidneys were grossly identifiable under general illumination in all examined *Pkd1*$^{L3/L3}$ mice older than 14 days (Figure 2E). However, this renal cystic disease was never found in *Pkd1*$^{L3/+}$ mice. To determine the development and progression of the polycystic kidney diseases in *Pkd1*$^{L3/L3}$ mice, we examined the kidney sections at embryonic days 13.5, 15.5, and 18.5, and postnatal days 1, 7, 14, 30, and 120 ($n$ = 6 at each age). Histologically, cystic dilation of renal tubules in outer medulla was first noticed at E15.5 (Figure 3A), consisting with the finding in *Pkd1*-null embryos. This was followed by progressive dilatation and cyst formation in renal tubules of the inner medulla and cortex (Figure 3, C and E). The number and size of the cysts increased with age until

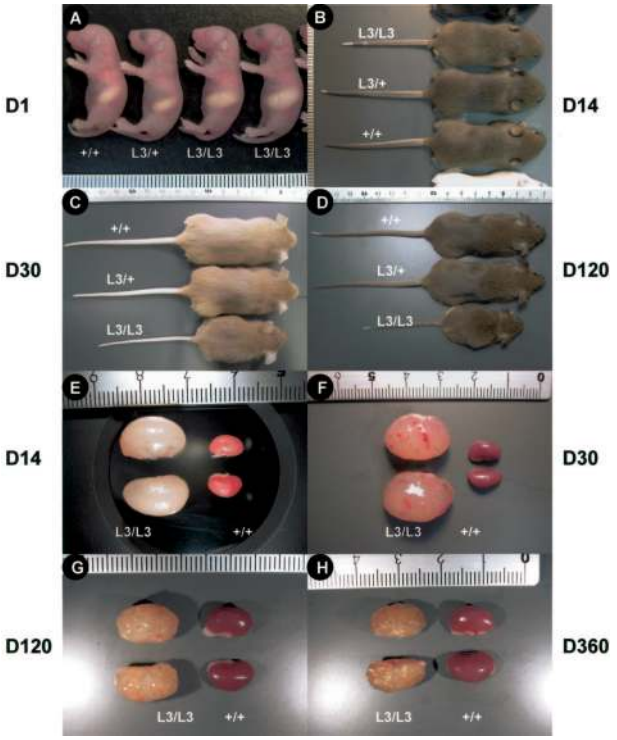


**Figure 2.** Postnatal growth retardation and kidney enlargement in *Pkd1*$^{L3/L3}$ mutant mice. **A–D:** Overall appearances of *Pkd1*$^{L3/L3}$ mutant mice and their control littermates at postnatal day 1 (**A**; D1), day 14 (**B**; D14), day 30 (**C**; D30), and day 120 (**D**; D120) are shown. The growth retardation and abdominal distention of *Pkd1*$^{L3/L3}$ mutant mice were first noticed at postnatal day 14. **E–H:** Gross morphologies of the kidneys of *Pkd1*$^{L3/L3}$ mutant mice and their control littermates at postnatal day 14 (**E**; D14), day 30 (**F**; D30), day 120 (**G**; D120), and day 360 (**H**; D360) are shown. The kidney enlargement in *Pkd1*$^{L3/L3}$ mutant mice was first observed at postnatal day 14 and continuously expanded thereafter. Notably, the enlarged kidneys began to regress after postnatal day 60. All results are representative of at least three mice per genotype in two independent experiments.

~30 days, and then many cysts began to diminish in size (Figure 3, G, I, and K). This finding is coincident with the gross changes in size and shape of kidney. The rate of cyst development indicates a less aggressive disease in *Pkd1*$^{L3/L3}$ mice than in homozygous *Pkd1*-null mice, thus providing evidence that the level of polycystin-1 has an impact on the disease progression. On postnatal day 14, epithelial cysts occupied the entire cortex and medulla of the affected kidney (Figure 3G). On postnatal day 30, larger and more massive cysts were found, surrounded by intact renal parenchyma with interstitial fibrosis and mild inflammation (Figure 3, I and J). On postnatal day 120, the numbers of the cysts larger than 300 $\mu$m dramatically decreased, accompanied by severe interstitial fibrosis (Figure 3, K and L). Glomerular cysts were rare at all times. Most of the tubular cysts were lined by monolayer epithelium ranging from cuboidal to hobnail or flattened; however, some expressed with multiple layers of epithelium. The manifestation of interstitial fibrosis was determined by Masson trichrome staining and first became evident at postnatal day 7 (Figure 3, B, D, and F). Another index of interstitial fibrosis of the tubulointerstitium in renal disease is the differentiation of the fibroblast to a myofibroblast. This may be quantitated by the immunohistochemical determination of $\alpha$-SMA. In the normal

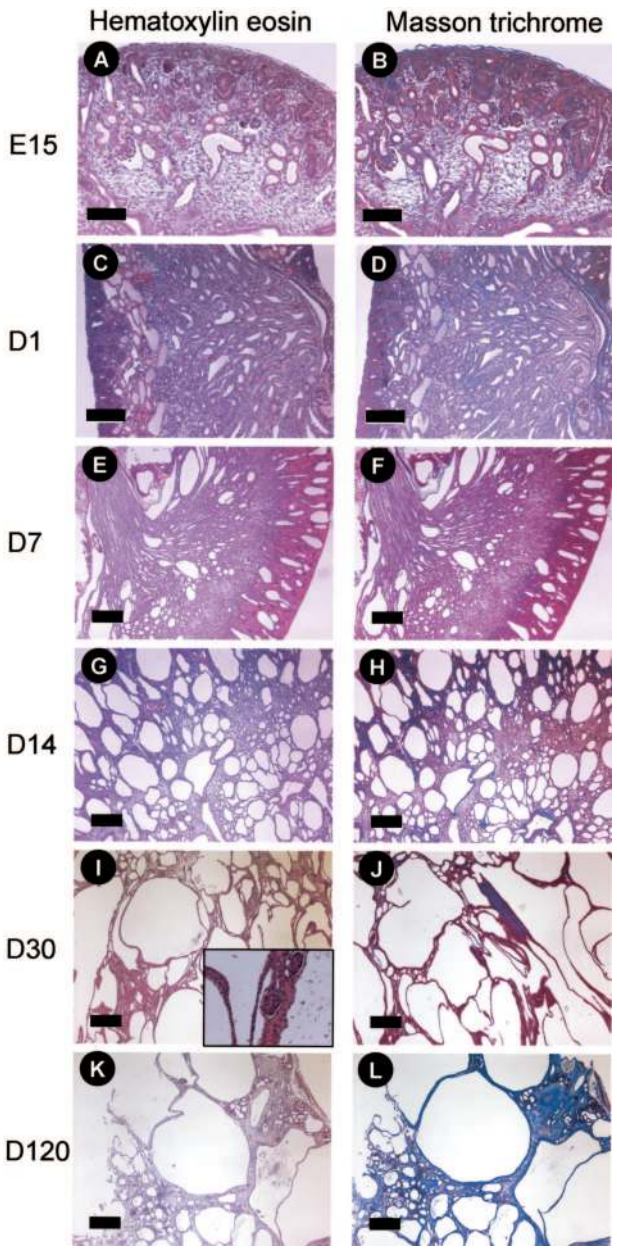


**Figure 3.** Progression of renal cystic lesions in *Pkd1*$^{L3/L3}$ mutant mice. **A**, **C**, **E**, **G**, **I**, **K:** H&E-stained kidney sections of embryonic day 15 (**A**; E15), postnatal day 1 (**C**; D1), day 7 (**E**; D7), day 14 (**G**; D14), day 30 (**I**; D30), and day 120 (**K**; D120) reveal the progression of renal cyst formation and enlargement in *Pkd1*$^{L3/L3}$ mutant mice. The renal cysts were homogenously distributed over the whole kidney and were accompanied with mild inflammation. Intact glomeruli and proximal tubules were still observed between enlarged cysts (**inset** in **I**). **B**, **D**, **F**, **H**, **J**, **L:** Masson-trichrome-stained kidney sections of embryonic day 15 (**B**; E15), postnatal day 1 (**D**; D1), day 7 (**F**; D7), day 14 (**H**; D14), day 30 (**J**; D30), and day 120 (**L**; D120) reveal significant temporal variation of interstitial collagen deposition as a hallmark of interstitial fibrosis, especially after D30. All results are representative of at least three mice per genotype in two independent experiments. Scale bars, 300 $\mu$m.

kidney (Figure 4, A–C), $\alpha$-SMA is primarily, if not exclusively, confined to the arteries and small vessels. In the kidney of *Pkd1*$^{L3/L3}$ mice, $\alpha$-SMA is also present in the widened interstitium (Figure 4, D–F) as well as in the blood vessels. The results of several individual animals of each genotype and age are summarized in Figure 4G, indicating the progression of renal interstitial fibrosis in mutant mice. Consistent with Masson trichrome staining, the significant increase in $\alpha$-SMA matrix score, as compared with wild-type mice, was first noticed at postnatal day 7, when the cysts had already formed for several days. These findings suggest that the interstitial fibrosis is a secondary complication of the renal cyst development.

## *Pkd1*$^{L3/L3}$ *Mice Show Growth Retardation and Early Mortality*

The *Pkd1*$^{L3/L3}$ mice are indistinguishable from their wild-type littermates in the early postnatal period. However, the mutant mice finally exhibited distended abdomens and short stature at weaning compared to their littermates. Approximately 50% of these mice died within 1 to 2 months after birth (Figure 5A). Bone defects were also found in *Pkd1*-null mutants, and this could have caused the growth retardation observed in newborn mice of those null mutants. The short stature of the *Pkd1*$^{L3/L3}$ mice was noticed beyond postnatal day 14 (Figure 5B), much later than those of *Pkd1*-null mutants. *Pkd1*$^{L3/L3}$ mice sacrificed after postnatal day 14 exhibited significant increases in percentages of kidney weight to body weight (Figure 5C) and kidney volumes (Figure 5D). These findings indicate kidney enlargement and massive renal cysts were presented as early as postnatal day 14, which could cause renal insufficiency leading to growth retardation and early mortality. Meanwhile, the high serum blood urea nitrogen levels indicated renal failure in these mutants (Figure 5E). In this regard, we suppose the short stature of the *Pkd1*$^{L3/L3}$ mice may be a secondary complication of the severe renal cystic disease. The other 50% homozygous survivals lived into adulthood with similar phenotype, and most of them died before 1 year of age (Figure 5A). Only five homozygous mice (~10%) were still alive at 1 year, and they were sacrificed for examination, showing renal cystic lesions in all these mice. Notably, most of these survivals became sterile adults under normal breeding conditions, even though mature sperms and follicles were observed in their sexual organs.

## *Proliferation and Apoptosis of Renal Cystic Epithelial Cells*

A precisely controlled balance between cellular proliferation and programmed cell death (apoptosis) is essential for normal growth and differentiation of the kidney and maintenance of normal renal structure after birth. These fundamental processes are disturbed in polycystic kidneys.[24,25] In an attempt to reveal these processes in our ADPKD mouse model, we estimated the mitotic and apoptotic indices using proliferating cell nuclear antigen (PCNA) immunohistochemistry and TUNEL staining, respectively. The increased mitotic index observed in renal epithelium of the *Pkd1*$^{L3/L3}$ mice with respect to control mice was found as expected, because cyst formation and expansion should be associated with overprolifera-

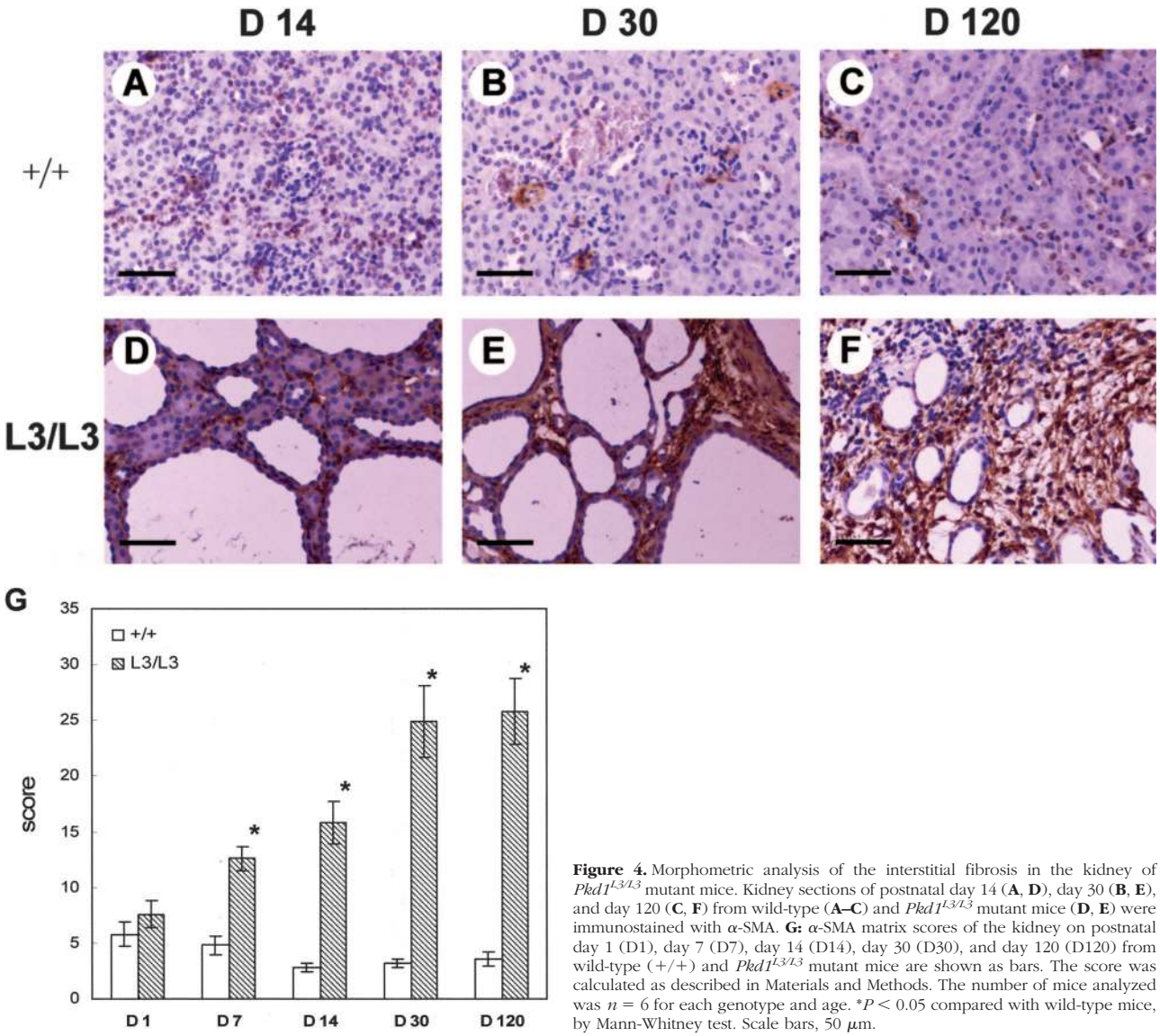


**Figure 4.** Morphometric analysis of the interstitial fibrosis in the kidney of $Pkd1^{L3/L3}$ mutant mice. Kidney sections of postnatal day 14 (**A**, **D**), day 30 (**B**, **E**), and day 120 (**C**, **F**) from wild-type (**A–C**) and $Pkd1^{L3/L3}$ mutant mice (**D**, **E**) were immunostained with α-SMA. **G:** α-SMA matrix scores of the kidney on postnatal day 1 (D1), day 7 (D7), day 14 (D14), day 30 (D30), and day 120 (D120) from wild-type (+/+) and $Pkd1^{L3/L3}$ mutant mice are shown as bars. The score was calculated as described in Materials and Methods. The number of mice analyzed was $n = 6$ for each genotype and age. $^*P < 0.05$ compared with wild-type mice, by Mann-Whitney test. Scale bars, 50 μm.

tion of the cyst-lining epithelium (Figure 6, A, B, and E). The boost in mitotic rate observed at postnatal day 14 correlated well with the massive cyst formation and rapid cyst expansion at this stage (Figures 3G and 6B). The drop in mitotic activity occurring after postnatal day 30 also coincided with the decrease in cyst formation thereafter. Notably, the temporal variation pattern of the mitotic index during kidney development was similar between normal and cystic kidneys (Figure 6E). This finding suggests that cell proliferation of the renal tubular epithelium in the affected kidney is still controllable during development, even though the mitotic rate is statistically significantly higher than those of wild-type kidney in all cases. The controllable proliferation predicted a nonmalignant phenotype of the renal tubular epithelium. The increased apoptotic index in renal epithelial cells of the cystic kidney was first noticed at postnatal day 30 and rose to ~85% at day 120 (Figure 6, C, D, and F). No excessive apoptosis occurred in the affected kidney before postnatal day 14, indicating that the alternation in cell apoptosis might not be involved in the pathogenesis of renal cyst formation and enlargement. A high apoptotic rate was observed only in the older affected kidney, where cyst formation decreases and cyst regression had began to appear, leading to shrinking of the kidney. This finding suggests a possible causal relationship between the augmenting apoptosis of cystic epithelial cells and the regression of renal cysts in the older affected kidney.

## *Segments of Origin of Renal Tubular Cysts*

We used known nephron segment-specific markers to specifically identify the origin of the renal tubular cysts. Lectin *Dolichos biflorus* specifically labels the collecting duct, the antibody directed against Tamm-Horsfall protein labels the thick ascending limb, and the antibody against lysozyme labels the proximal tubule. Interestingly, the majority of renal cysts stained positively for the more distal portion markers, where none was positive for

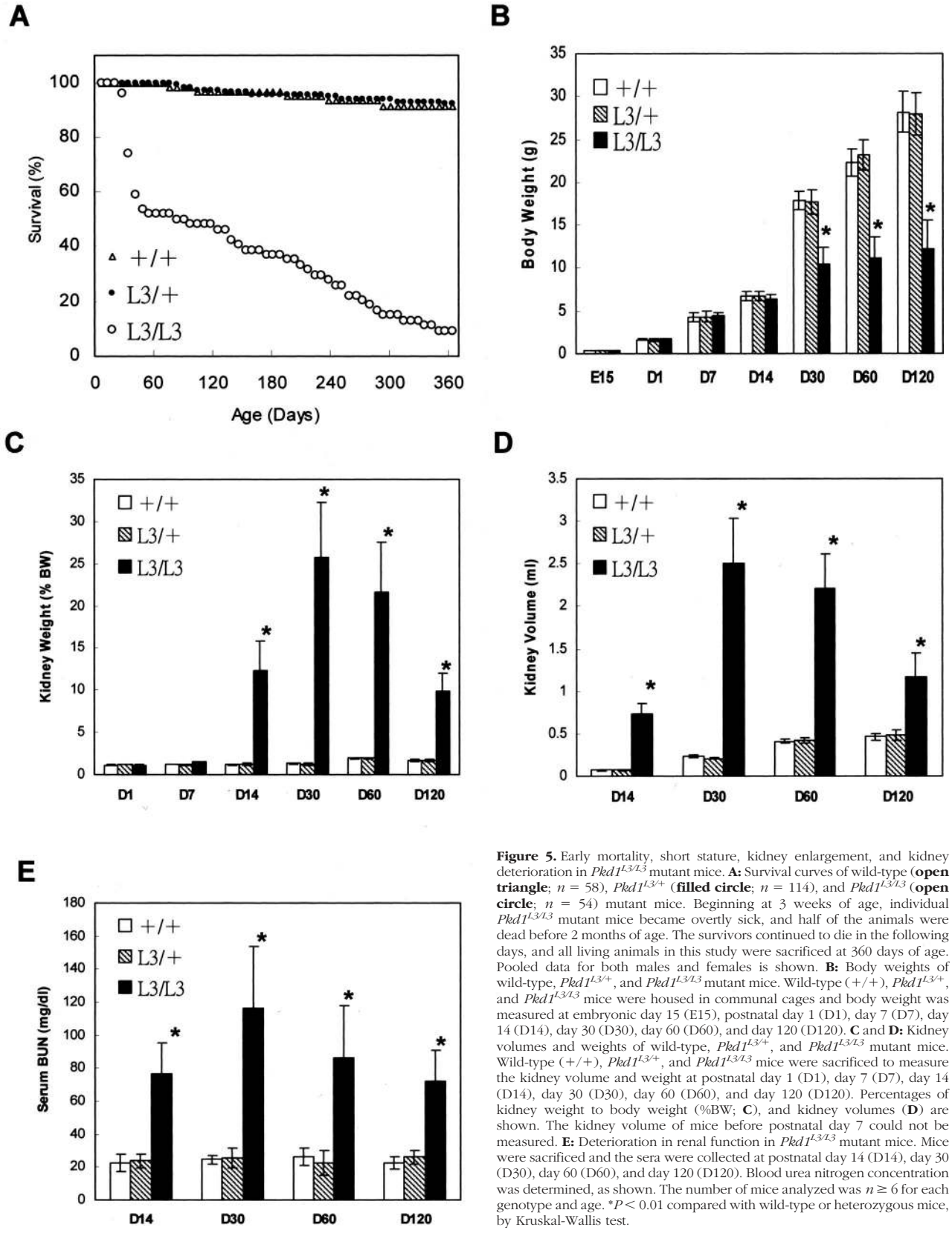


**Figure 5.** Early mortality, short stature, kidney enlargement, and kidney deterioration in *Pkd1*$^{L3/L3}$ mutant mice. **A:** Survival curves of wild-type (**open triangle**; $n = 58$), *Pkd1*$^{L3/+}$ (**filled circle**; $n = 114$), and *Pkd1*$^{L3/L3}$ (**open circle**; $n = 54$) mutant mice. Beginning at 3 weeks of age, individual *Pkd1*$^{L3/L3}$ mutant mice became overtly sick, and half of the animals were dead before 2 months of age. The survivors continued to die in the following days, and all living animals in this study were sacrificed at 360 days of age. Pooled data for both males and females is shown. **B:** Body weights of wild-type, *Pkd1*$^{L3/+}$, and *Pkd1*$^{L3/L3}$ mutant mice. Wild-type (+/+), *Pkd1*$^{L3/+}$, and *Pkd1*$^{L3/L3}$ mice were housed in communal cages and body weight was measured at embryonic day 15 (E15), postnatal day 1 (D1), day 7 (D7), day 14 (D14), day 30 (D30), day 60 (D60), and day 120 (D120). **C** and **D:** Kidney volumes and weights of wild-type, *Pkd1*$^{L3/+}$, and *Pkd1*$^{L3/L3}$ mutant mice. Wild-type (+/+), *Pkd1*$^{L3/+}$, and *Pkd1*$^{L3/L3}$ mice were sacrificed to measure the kidney volume and weight at postnatal day 1 (D1), day 7 (D7), day 14 (D14), day 30 (D30), day 60 (D60), and day 120 (D120). Percentages of kidney weight to body weight (%BW; **C**), and kidney volumes (**D**) are shown. The kidney volume of mice before postnatal day 7 could not be measured. **E:** Deterioration in renal function in *Pkd1*$^{L3/L3}$ mutant mice. Mice were sacrificed and the sera were collected at postnatal day 14 (D14), day 30 (D30), day 60 (D60), and day 120 (D120). Blood urea nitrogen concentration was determined, as shown. The number of mice analyzed was $n \geq 6$ for each genotype and age. *$P < 0.01$ compared with wild-type or heterozygous mice, by Kruskal-Wallis test.

the proximal tubular marker (Figure 7). The tubular structures positive for lysozyme were still found in renal parenchyma surrounding cysts (Figure 7, G and H), validating our staining results. Most *Pkd1* mutant mice and ADPKD patients have renal cysts of proximal tubule origin even though the renal cysts arise mainly from the

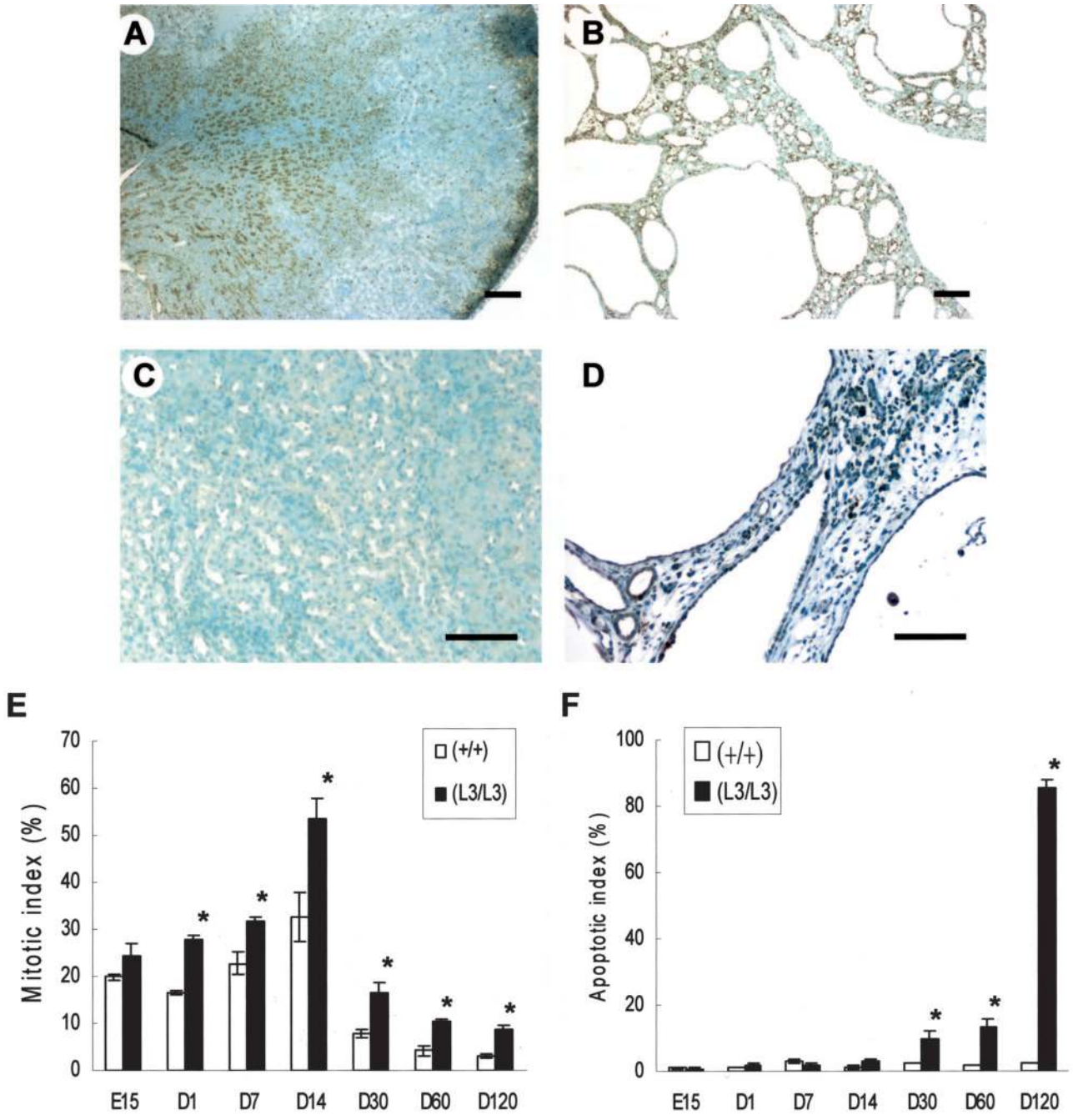


**Figure 6.** Alternations in proliferation and apoptosis of renal epithelial cells in *Pkd1*$^{L3/L3}$ mutant mice. Kidney sections at embryonic day 15 (E15), postnatal day 1 (D1), day 7 (D7), day 14 (D14), day 30 (D30), and day 120 (D120) from wild-type and *Pkd1*$^{L3/L3}$ mutant and wild-type mice were prepared. Immunostaining for PCNA, using monoclonal antibodies (Upstate Biotechnology, Lake Placid, NY), and the TUNEL assay, using the ApopTag peroxidase *in situ* apoptosis detection kits (Vectastain; Vector Elite, Burlingame, CA), were used to measure proliferation and apoptosis. Kidney sections of postnatal day 14 from wild-type (**A**) and *Pkd1*$^{L3/L3}$ (**B**) mutant mice stained with PCNA, and of postnatal day 120 from wild-type (**C**) and *Pkd1*$^{L3/L3}$ (**D**) mutant mice stained with TUNEL are illustrated. Fields (×400) of renal section were randomly selected and all of the epithelial cells were characterized regardless of their localization in cyst or tubule. At least 500 epithelial cells per tissue were counted. The mitotic (**E**) and apoptotic (**F**) indices were calculated as the percentage of cells positive for PCNA and TUNEL assay, respectively. The number of mice analyzed was $n \geq 4$ for each genotype and age. $^*P < 0.05$ compared with wild-type mice, by Mann-Whitney test. Scale bars, 100 $\mu$m.

distal portion of renal tubular segments. The negative staining of the renal cysts with a single proximal tubular marker could not definitely exclude proximal cyst formation. In addition, some cysts were negative for all markers. These cysts could be derived from any segment of nephron including proximal tubule, and loss of these tubular markers suggests a degree of dedifferentiation. We further estimated percentages of the renal cysts exhibiting the nephron segment-specific markers in various ages of *Pkd1*$^{L3/L3}$ mice, as summarized in Table 1. A mean 75.83% of cysts were positive for collecting duct, 2.83% for thick ascending limb, and 2.17% for both markers in the early stage of cyst formation. The cysts that stained positive for both markers could be derived from

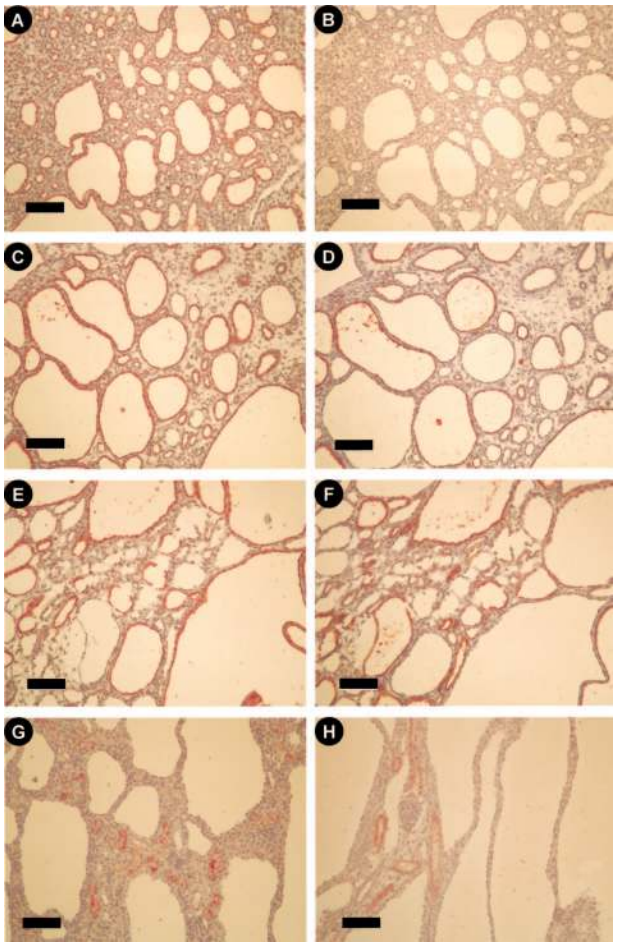


**Figure 7.** Cysts arise from distal nephron segments. Kidney sections of postnatal day 7 (**A**, **B**), day 14 (**C**, **D**, **G**), and day 30 (**E**, **F**, **H**) from *Pkd1*$^{L3/L3}$ mutant mice were stained with *Dolichos biflorus* lectin (**A**, **C**, **E**), a collecting duct-specific lectin, stained with Tamm-Horsfall protein antibodies (**B**, **D**, **F**), a specific marker for thick ascending limb, and stained with antibodies to lysozyme (**G**, **H**), a specific marker for proximal tubule. Most cysts were positively stained with specific markers of collecting ducts and thick ascending limbs. Lysozyme-positive cysts were not found, and intact proximal tubules were stained positively with this specific marker. Notably, some cysts were negative for all these specific markers, suggesting the characterization of undifferentiation and/or dedifferentiation of the cyst-lining epithelial cells. All results are representative of at least three mice per genotype in two independent experiments. Scale bars, 100 $\mu$m.

the connecting segment between thick ascending limb and collecting duct. During progression of the renal cystic disease, the ratios of cysts positive for collecting duct gradually decreased from 75.67% on postnatal day 14 to 50.50% on day 30 (Figure 7, C and E). Conversely, the ratios for thick ascending limb and the connecting segment increased from 7.50% to 21.50% and from 4.00% to 17.50%, respectively (Figure 7, D and F). At postnatal day 120, the ratios for collecting duct had reduced to 43.83%, for thick ascending limb had increased to 29.17%, and for the connecting segment had increased to 23.83%. These results reveal that the collecting ducts begin to develop cysts in the early postnatal period, and the connecting segment and thick ascending limb develop cysts mainly in the later stages.

## *Signaling of Epidermal Growth Factor Receptor in Renal Cystic Epithelium*

It is now well accepted that cell proliferation is an essential component of cyst formation; however, it is not clear what drives this proliferation. Because epidermal growth factor (EGF) is a well-known agent that stimulates cell proliferation in primary cultured renal tubular cells and ADPKD cells,[26] we examined EGF signaling in the renal cystic epithelium of the *Pkd1*$^{L3/L3}$ mice. We first determined the EGF expression levels in the kidneys of postnatal day 30 by RT-PCR and found that the EGF transcript did not increase as predicted but instead decreased in the kidneys of the homozygous *Pkd1*$^{L3/L3}$ mice (Figure 8A). Previous studies found that expression of an EGF-related growth factor called HB-EGF increased in the rat kidney after acute ischemic insult and that HB-EGF was also expressed predominantly in the ureteric bud during rat metanephric development.[27] These results suggest that HB-EGF seems to stimulate cell proliferation during kidney development and regeneration. In addition, HB-EGF has been reported to play an important role in stimulating cell proliferation of cystic and normal collecting tubular epithelia.[28] Significantly, the HB-EGF expression in affected kidney of *Pkd1*$^{L3/L3}$ mice was found to increase after normalization with $\beta$-actin expression (Figure 8A). HB-EGF binds to and activates EGF-receptor (EGFR) with an even greater effect than EGF. We hence determined the expression level and activation degree (as assessed by EGFR phosphorylation) of EGFR by Western blot analysis. Both total protein content and phosphorylation form of EGFR increased 5- to 10-fold in homozygous *Pkd1*$^{L3/L3}$ mice, compared with wild-type or heterozygous mice, respectively (Figure 8B). In contrast, the protein level of an EGFR-related receptor tyrosine kinase erbB2, which is not bound and activated by HB-EGF, increased only approximately twofold in affected

**Table 1.** Percentages of the Renal Cysts Exhibiting Nephron Segment-Specific Markers in Various Ages of PKD$^{L3/L3}$ Mice

| Marker (nephron segment) | Mouse age | | | |
|---|---|---|---|---|
| | Day 7 | Day 14 | Day 30 | Day 120 |
| Lysozyme (PT) | 0 | 0 | 0 | 0 |
| Tamm-Horsfall protein (TAL) | 2.83 ± 1.57 | 7.50 ± 3.25 | 21.50 ± 8.73 | 29.17 ± 9.18 |
| Lectin *Dolichos biflorus* (CD) | 75.83 ± 17.42 | 75.67 ± 12.36 | 50.50 ± 7.90 | 48.83 ± 9.61 |
| Positive staining for both TAL and CD | 2.17 ± 1.21 | 4.00 ± 2.31 | 17.50 ± 5.82 | 23.83 ± 5.73 |

Renal cysts smaller than 50 mm in diameter were excluded from the total count. In individual cyst, more than half of the cyst-lining epithelial cells labeled with specific markers was defined as positive staining. Two hundred renal cysts were determined in each specimen, and each data represents the mean ± SE from three independent mice. PT, proximal tubule; TAL, thick ascending limb; CD, collecting duct.

kidneys (Figure 8B). The fractions of membrane-bound Grb2 and Shc, which indirectly represent the mediators recruited by activated EGFR during signaling, also clearly increased in affected kidneys (Figure 8B). Finally, the EGFR in cystic epithelial cells was mislocalized to apical membranes (Figure 8C). The enrichment of EGFR signaling was also evidenced in *Pkd1*$^{L3/L3}$ mice at postnatal days 14 and 60 but not at postnatal day 7, as assessed by RT-PCR and Western blot analysis (data not shown). However, the overexpression and mislocalization of EGFR in renal cystic epithelia also was visible at postnatal day 7 by immunohistochemistry analysis (data not shown). Taken together, the enhancement and mislocalization of EGFR signaling may be early markers of cystic transformation in *Pkd1* insufficiency and could be responsible for the overproliferation of the renal cystic epithelial cells.

## $Na^+/K^+$-ATPase, Aquaporin-2, cAMP, and Vasopressin V2 in Renal Cysts

Fluid accumulation in renal cysts is the other main manifestation of polycystic kidney. The net reabsorption of fluid in the normal kidney is brought about by sodium ion gradients established by the $Na^+/K^+$-ATPase in the basolateral tubular cell membrane and by multiple ion and fluid transporters and channels in apical and basolateral sites. The $Na^+/K^+$-ATPase is composed of $\alpha$1 and $\beta$1 subunits in normal adult kidneys and is highly expressed in the thick ascending limb and the distal convoluted tubule.[29] The protein content of either the $\alpha$1 or $\beta$1 subunit of $Na^+/K^+$-ATPase in cystic kidney was clearly lower than in normal kidneys (Figure 8D). In contrast, the content of $Na^+/K^+$-ATPase $\beta$2 subunit was clearly increased in cystic kidneys (Figure 8D). Because the $\beta$2 subunit is highly expressed in normal fetal kidneys, this finding suggests a degree of either undifferentiation or dedifferentiation in the renal cystic epithelium. The distribution of the $Na^+/K^+$-ATPase $\alpha$1 subunit in normal kidneys was mainly localized in the outer medulla region, where it was concentrated at the basolateral sites of the epithelial cells (Figure 8F). Interestingly, the $Na^+/K^+$-ATPase was undetectable in almost all epithelial cells lining large cysts, although it was still present in a few small cysts and weakly expressed in some normal renal tubule in affected kidneys of 30-day-old mice (Figure 8G). At this stage, ~20% of cysts were derived from the thick ascending limb and the connecting segment where $Na^+/K^+$-ATPase was highly expressed in normal kidneys. Our results indicate that the down-regulation of $Na^+/K^+$-ATPase $\alpha1\beta1$ complex in cystic epithelial cells may diminish the *trans*-epithelial sodium gradients, leading to fluid accumulation in renal cysts. Recently, increased cAMP levels and up-regulation of vasopressin V2 receptor (VPV2R) as well as a water channel aquaporin-2 have been identified as playing an important role in the pathogenesis of an ADPKD mouse model derived from somatic inactivation of *Pkd2*.[30] In our model, aquaporin-2 and VPV2R were also overexpressed in the cystic kidney (Figure 8, A and D). The increased cAMP in renal cysts was also observed (Figure 8E), suggesting the similarity between these two different ADPKD mouse models.

## Extrarenal Abnormalities in *Pkd1*$^{L3/L3}$ Mice

Cardiac septal defects, pulmonary hypoplasia, and severe cystic manifestations in hepatic and pancreatic ducts are usually found in some homozygous *Pkd1*-targeted mutants, indicating the essential roles of polycystin-1 in developing and maintaining the architecture of these organ systems. In our *Pkd1*$^{L3/L3}$ mice, hepatic cysts were never found and pancreatic cysts were observed only rarely, in two of the examined mice (age, 120 and 360 days). The weights of lung and heart (percent of body weight) were still normal, even though the body weights were dramatically lower than those of wild-type mice. The histological examinations of aorta, lung, and heart also appeared to be normal. The levels of *Pkd1* transcript and protein in heart, liver, lung, and pancreas were also determined by RT-PCR and Western blot, as described above. We found that the *Pkd1* transcript in these organs of *Pkd1*$^{L3/L3}$ mice was also clearly lower than in those of *Pkd1*$^{L3/+}$ and wild-type mice, similar to the finding in the kidney (data not shown). These findings suggest that the interfering effect of the intronic *mc1-neo* on *Pkd1* expression is ubiquitous in many tissues. Although the *Pkd1* transcript could be determined, the polycystin-1 protein in these organs was undetectable (data not shown). Only the kidney can express detectable amounts of polycystin-1 protein, no matter whether in embryos, neonates, or adult mice (data not shown). The relative abundance of polycystin-1 expression implicates the high-level requirement of this crucial protein in the kidney compared to the other organ systems. The low levels of native polycystin-1 in *Pkd1*$^{L3/L3}$ mice was sufficient to prevent these common defects in the other organs caused by *Pkd1*-null mutation, but it failed to provide a similar effect in the kidney.

## Discussion

Our findings provide clear evidence that diminished expression of native polycystin-1 is sufficient to induce the renal cystic lesions of ADPKD. We showed that the intronic insertion of *neo* gene in reverse orientation into *Pkd1* could intensively interfere in transcription and/or splicing machinery, resulting in a low but not completely null *Pkd1* expression. Only wild-type *Pkd1* transcript and protein were detected in either heterozygous *Pkd1*$^{L3/+}$ or homozygous *Pkd1*$^{L3/L3}$ mice. No mutant *Pkd1* transcript in mRNA was detected in heterozygotes and homozygotes by RT-PCR analysis using two more sets of primers located in exon 34 and exon 35 (data not shown). These findings suggest that the intronic *neo* is not inserted into the neighboring *Pkd1* transcript. The hypomorphic allele published here is a totally pure knockdown allele for *Pkd1*, representing only a lower-than-normal level of expression without mutant transcript expression. This outstanding knockdown allele could be very informative in exploring the biological function of polycystin-1 without

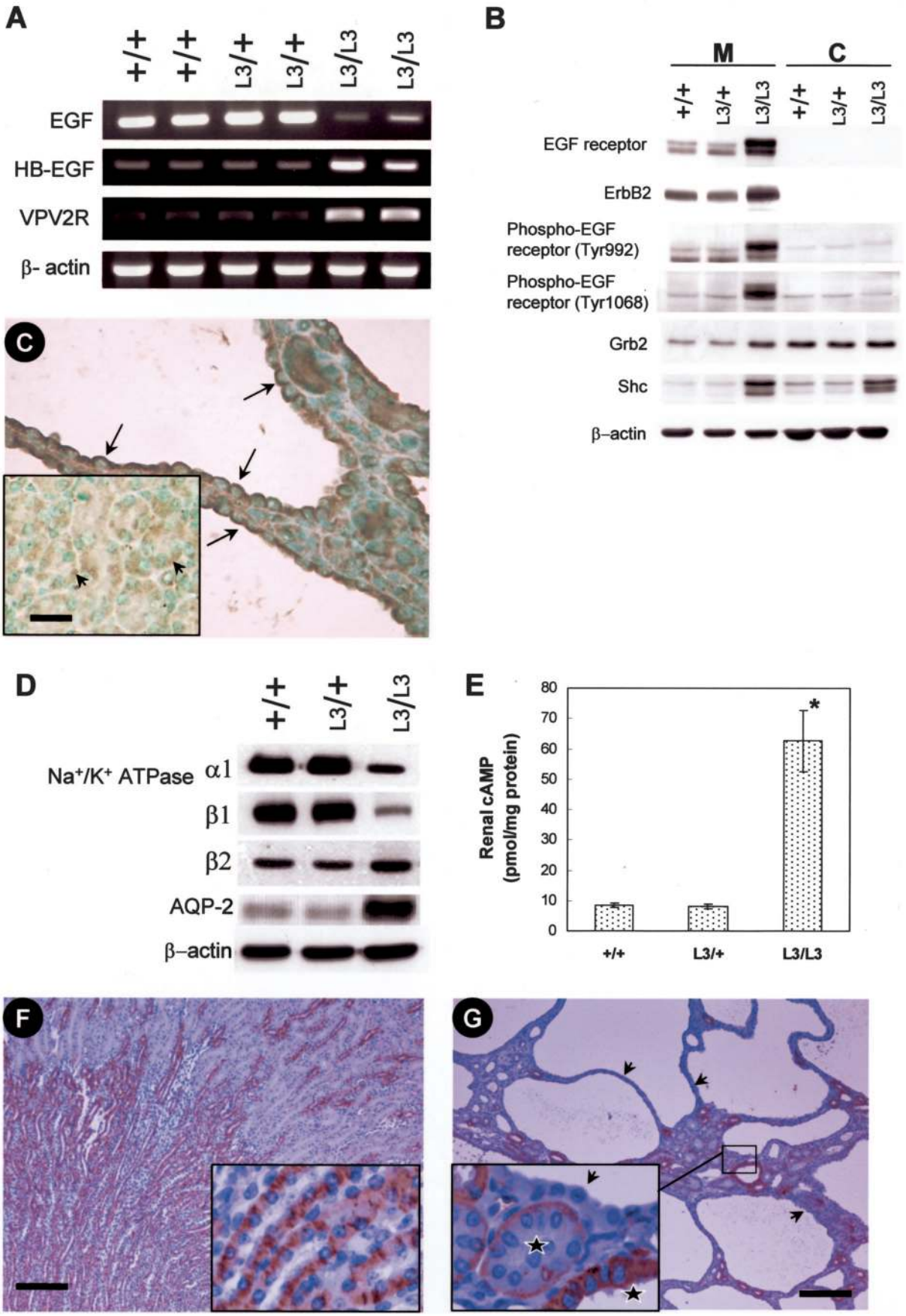
A
+/+
+/+
L3/+
L3/+
L3/L3
L3/L3
EGF
HB-EGF
VPV2R
β- actin
B
M
C
+/+
L3/+
L3/L3
+/+
L3/+
L3/L3
EGF receptor
ErbB2
Phospho-EGF receptor (Tyr992)
Phospho-EGF receptor (Tyr1068)
Grb2
Shc
β–actin
C
D
+/+
L3/+
L3/L3
Na+/K+ ATPase α1
β1
β2
AQP-2
β–actin
E
Renal cAMP (pmol/mg protein)
80
70
60
50
40
30
20
10
0
*
+/+
L3/+
L3/L3
F
G

the interference caused by the mutant protein. The mutant mouse homozygous for the knockdown allele is a crucial animal model for the study of ADPKD.

The observation that mice with homozygous targeting disruption of *Pkd1* die *in utero* during the later stages of gestation suggests that polycystin-1 is essential for normal development. These mouse models have similar patterns of renal development, with grossly normal patterns of ureteric bud branching and mesenchymal induction. Abruptly, around E15, cystic structures arise in the medulla, suggesting that polycystin-1 is required for the final maturation of renal epithelia. In the present study, the low levels of native polycystin-1 in $Pkd1^{L3/L3}$ mice are sufficient to overcome the embryonic and perinatal lethality usually observed in *Pkd1*-targeted disruption mutants. But the $Pkd1^{L3/L3}$ mice still begin to develop renal tubular dilatation at embryonic day 15.5, identical with the finding in *Pkd1*-targeted disruption mutants. However, they progress to severe renal cystic disease in a milder manner than the other targeted mutants. Renal tubular dilation was widely present in the early stage, and the renal cysts emerged gradually and continuously later. The polycystin-1 levels in kidneys of the $Pkd1^{L3/L3}$ mice are shown to be ~80% lower than those in the wild-type mice, suggesting that the remaining ~20% of polycystin-1 is not sufficient to prevent the initiation but could be responsible for the delay in progression of the renal cystic disease. These results demonstrate the quantity requirement of polycystin-1 in both maturating and maintaining the renal tubular architecture. This conclusion is concordant with studies indicating that polycystin-1 expression in renal epithelia peaks between E16 and E19 and remains elevated until tubular maturation is complete in neonatal life.[31] Thereafter, expression declines to lower levels in the adult.[19,20] The variation in *Pkd1* expression level indicates that the difference in polycystin-1 quantity required for maturating and maintaining the renal tubular architecture is higher for maturating and lower for maintaining. This could explain the utility of the remaining polycystin-1 only in retarding but not in initiating the renal cystic disease.

In human ADPKD, most cysts arise from the distal portion of renal tubular segments. Glomerular cysts are not usually a characteristic feature of adult ADPKD and are only observed in severe early onset cases.[32,33] In homozygous *Pkd1*-null mutants, renal cysts are originated from glomeruli and all tubular structures suggesting the critical role of polycystin-1 in all segments of nephron.[11] It is still unclear why the renal cysts arise mainly in distal segments in ADPKD. In our homozygous *Pkd1* knockdown mice, renal cysts developed mainly in distal portions of nephron. Intact glomeruli and proximal tubules still appeared, suggesting that the remaining polycystin-1 is still sufficient for maturating and maintaining the normal structure of glomeruli and proximal tubules. However, the remaining polycystin-1 could not allow the distal segments of nephron to develop normal architectures. These results indicate that the polycystin-1 quantity requirement for distal segments is obviously higher than for glomeruli and proximal segments. Moreover, the renal cysts are derived mainly from collecting duct in the early postnatal period. Even though the ratios of collecting duct cysts to thick ascending limb cysts significantly decrease with increasing age, this could be caused by the progressive apoptosis of the aged cysts developing from early postnatal period. These results suggest that the polycystin-1 quantity requirement for collecting duct could be higher than for other distal segments. This conclusion is concordant with the previous study showing that the highest polycystin-1 expression is found in collecting ducts and the other distal nephrons express a moderate level.[34] Expression in the proximal nephron is undetectable. Taken together, the high potentiality of the renal distal segments for cyst formation could be attributed to the high polycystin-1 quantity requirement for these segments.

ADPKD is an autosomal dominant disorder of late age onset characterized by focal cyst development and expansion, typically resulting in end-stage renal disease in late middle age. The severity of the disease, the age of onset of end-stage renal disease, and the spectrum of extrarenal manifestations vary widely between affected individuals, even within the same family.[35] A two-hit hypothesis has been proposed to explain many features of this disease including the focal cyst formation, late onset, loss of heterozygosity in cystic epithelial cells, and variability in the phenotype.[8,13] Basically, this hypothesis demonstrates a loss-of-function mechanism for cyst formation in ADPKD. ADPKD mouse models derived from targeted disruption of *Pkd1* also support this loss-of-function mechanism. But it still has some defects, such as its failure to identify somatic mutations in the majority of

**Figure 8.** Signaling of epidermal growth factor receptor (EGFR), cAMP concentrations, and expression of $Na^+/K^+$-ATPase as well as aquaporin-2 and vasopressin V2 receptor (VPV2R) in $Pkd1^{L3/L3}$ mouse kidneys. **A:** Overexpression of HB-EGF and VPV2R mRNA, and low expression of epidermal growth factor (EGF) in $Pkd1^{L3/L3}$ mouse kidneys. RNA was extracted from mouse kidneys of postnatal day 30 and mRNA levels were determined by RT-PCR. Amplification of $\beta$-actin shows the equivalence of the RNA loading and amplification. **B:** Overexpression and activation of EGFR protein in $Pkd1^{L3/L3}$ mouse kidneys. The renal levels of depicted proteins in membrane (M) and cytosol (C) fractions of postnatal day 30 were determined by Western blot analysis. $\beta$-Actin was used as loading control for equivalent content of protein. **C:** EGFR mislocalization in renal cystic epithelia of $Pkd1^{L3/L3}$ mouse kidneys. Renal sections of postnatal day 30, immunostained with EGFR antibodies reveal the apical (**arrows**) and basal (**arrowheads** in **inset**) localization in $Pkd1^{L3/L3}$ and wild-type mice, respectively. **D:** Overexpression of aquaporin-2 (AQP-2) and low expression of adult form $Na^+/K^+$-ATPase in $Pkd1^{L3/L3}$ mouse kidneys. The levels of depicted proteins in kidney membrane fraction of postnatal day 30 were determined by Western blot analysis. $\beta$-Actin was used as loading control. **E:** Renal concentrations of cAMP, measured using enzyme immunoassay and expressed per mg of protein, in 30-day-old wild-type as well as $Pkd1^{L3/+}$ and $Pkd1^{L3/L3}$ mice. The enzyme immunoassay kit (catalog no. 581001) was obtained from Cayman Chemical (Ann Arbor, MI). The number of mice analyzed was $n = 6$ for each genotype. $^*P < 0.01$ compared with wild-type or heterozygous mice, by Kruskal-Wallis test. **F:** Localizations of $Na^+/K^+$-ATPase $\alpha$-chain in wild-type mouse kidneys. Kidney sections of postnatal day 30 immunostained with antibodies against $Na^+/K^+$-ATPase $\alpha$-chain reveal basal lateral localization in renal epithelial cells of medullar region. **G:** Localizations of $Na^+/K^+$-ATPase $\alpha$-chain in $Pkd1^{L3/L3}$ mouse kidneys. Low or even absent expression of $Na^+/K^+$-ATPase $\alpha$-chain is revealed in epithelial cells lining large cysts (**arrowheads**). The basal lateral localization of $Na^+/K^+$-ATPase $\alpha$-chain is also found in tubular and small cystic epithelial cells (**asterisks**). The **insets** show high-power fields of the depicted area. All results are representative of at least three mice per genotype in two independent experiments. Scale bars, 20 $\mu$m.

cysts and expression of full-length polycystin-1 in a subset of cysts in kidneys of ADPKD patients with an inheritable defect in *PKD1*. These findings may be defended in part by acquiring undetected missense mutations in *PKD1*, resulting in mutant but still full-length polycystin-1 expression. However, no hot-spot for missense mutations has been identified. In this regard, some other genetic mechanisms, such as haploinsufficiency or dominant-negative mutations, should not be excluded, and multiple mechanisms are likely to be involved. For example, it has been shown that cysts can have *trans*-heterozygous mutations, in which individuals that carry a germline mutation of *PKD1* acquire a second hit in *PKD2*, and vice versa.[9,36] Mice with *trans*-heterozygous mutations of *Pkd1* and *Pkd2* exhibit more severe renal cystic disease than would be predicted by a simple additive effect of the cyst formation in singly heterozygous mice.[37] This gene dose effect is called haploinsufficiency, which may also play a role in the molecular mechanism of the ADPKD. Briefly, null mutations of a single allele in a diploid organism could decrease the probability of gene expression resulting in more variation in expression levels.[38] It is possible that ADPKD results from single allele null mutations that cause a finite lifetime risk for the *PKD* gene product to fall below a critical threshold because of increased variance in expression level with the remaining wild-type allele. This haploinsufficiency hypothesis explains many features of ADPKD, such as the focal nature, late onset, and variance in severity. However, it is still unclear whether low *PKD* expression is sufficient to initiate renal cyst formation.

In the present study, totally pure *Pkd1* knockdown mice were generated, demonstrating that the low *Pkd1* expression is sufficient to induce renal cyst formation. Our findings further support the haploinsufficiency mechanism in ADPKD. In addition, we postulate that any genetic or environmental factors involved in *Pkd1* down-regulation may incite renal cyst formation. This is another possible mechanism underlying the etiology of ADPKD. Indeed, considerable intrafamilial variability in the severity of renal cystic disease in the major form of ADPKD (PKD1) has been observed, reflecting the influences of genetic modifiers and environmental factors. At present, nothing is known about the molecular mechanisms regulating the normal expression of the PKD1 gene or whether transcriptional deregulation of the PKD1 gene has a role in cyst formation. This is an important topic in this field for future study. Nevertheless, analysis of ADPKD tissue has revealed persistent, or even enhanced, polycystin-1 immunoreactivity of cystic epithelia in most cysts.[14,19,20] This finding appears at odds with the requirement for inactivating or decreasing *PKD1* expression to initiate cystogenesis. Interestingly, polycystin-1 localization in normal kidneys is seen in the apical-lateral membranes of collecting duct epithelial cells.[17,39] Consistent with these results, polycystin-1 has been identified in cell junctional complexes and the single primary nonmotile cilia.[18,40,41] But in cystic tubule epithelial cells, polycystin-1 is predominantly cytoplasmic in its distribution suggesting the abnormal function. The similar or even high level of polycystin-1 expressed in renal cyst-lining epithelial cells could be functionally inactive. It is worthwhile considering the possible causes contributing to the loss of polycystin-1 function in ADPKD cysts. This may provide important clues to delineate the possible molecular mechanism involved in the pathogenesis of ADPKD. Calcium and polycystin-1 phosphorylation status are two of these possible factors involved in regulation of polycystin-1 function.[42,43] Altogether, the data support the postulation that either depletion of *PKD1* expression or loss of polycystin-1 function serves as an important trigger in cystogenesis.

Polycystic kidney disease is characterized by the enlargement of renal cysts, interstitial fibrosis, and gradual loss of normal renal tissue in association with progressive deterioration of renal function. In our homologous *Pkd1* knockdown mice, renal epithelia have an increased rate of proliferation simultaneous with cyst formation and enlargement. The overproliferation of renal epithelia is connected with the increased EGFR signaling. This finding is consistent with the phenotype observed in both human patients and several different mouse models of ARPKD.[26,44] For instance, EGFR antagonists have been widely tested as potential therapeutic interventions. But the effects are controversial, depending on the animal model used, and they have not yet been demonstrated in a *Pkd1* mouse model. The major ligand for EGFR in renal cysts was further identified as HB-EGF but not EGF. HB-EGF is a more potent mitogen for renal epithelia than EGF and is expressed mainly in the embryonic stage. This is a novel finding in the ADPKD mouse model, although similar results have been described in an ARPKD mouse model.[28] However, the role of HB-EGF in the cystogenesis needs to be further investigated in either ADPKD patients or a mouse model.

Both epithelial cell proliferation and fluid accumulation are responsible for cyst growth in ADPKD. A major and pathophysiologically significant abnormality in ADPKD cystic epithelia is the mispolarization of a fully functional $Na^+/K^+$-ATPase to the apical membranes of cyst epithelia.[45] This in turn is associated with basal-to-apical sodium ion transport leading to luminal fluid accumulation. Although apical mislocalization of the $Na^+/K^+$-ATPase has been reported in several different models of polycystic kidney disease,[46] it has not been universally accepted as the principal mechanism underlying either fluid secretion or cyst expansion in ADPKD. Immunocytochemical analysis of renal cysts with antibodies directed against $Na^+/K^+$-ATPase failed to detect evidence of apical mislocalization. $Na^+/K^+$-ATPase was expressed exclusively on the basolateral membranes. Expression levels of $Na^+/K^+$-ATPase dramatically decreased but were never mislocalized. Our data do not support the model of apical $Na^+/K^+$-ATPase-mediated, sodium-driven cyst fluid secretion. Indeed, Brill and colleagues[47] reported that they could not find evidence of mislocalization of $Na^+/K^+$-ATPase in either excised human ADPKD cysts or human ADPKD cyst cells in culture. The cyst luminal fluid accumulation may be driven by net basal-to-apical $Cl^-$ movements in a manner similar to that observed in classical secretory epithelia, such as sweat ducts or the airway,

rather than by apical secretion of $Na^+$. In this ion transporter system, apical $Cl^-$ exit could be facilitated by the cystic fibrosis transmembrane regulator (CFTR) protein, and the basolateral entry step may be mediated by the $Na^+$-$K^+$-$2Cl^-$ co-transporter NKCC1. In an attempt to delineate the possible pathway for cyst fluid secretion, in the near future we will determine the expression level and localization of some channels and transporters in ADPKD mice.

The process causing the progressive loss of renal tissue is unknown, but it could be the result of a form of programmed cell death known as apoptosis. Significant quantities of apoptotic cells have been reported both in ARPKD and in ADPKD;[25] however, whether this apoptosis is involved directly in cyst formation and/or loss of renal function is as yet undetermined. With the use of TUNEL staining, we have found the presence of apoptotic bodies in renal cystic epithelia of the homozygous *Pkd1* knockdown mice only after postnatal day 30, and the ratio of apoptotic cells successively increased thereafter. Since the massive renal cysts have already developed at postnatal day 14, apoptotic bodies are rarely found before that time. The increased apoptotic cell death does not seem to be strictly required in the cystogenesis. However, the cystic epithelia presented extensive apoptotic bodies at the late stage when the enormous cysts had shrunk and interstitial fibrosis was typical. The connection between cell apoptosis and cyst shrinking is logical. Although the exact death cues responsible for cell apoptosis in well-expanding cysts remain to be identified, there are some candidates that could trigger an apoptotic program in the tubular cells. For example, infiltration of inflammatory cells as seen in the cystic kidneys may contribute to cell death by producing prodeath ligands or cytokines.[48] Likewise, in cystic kidneys with persistent pressure on interstitial tissue, chronic hypoxia induced by a compromised interstitial blood flow could result in cellular ATP deprivation, which might serve as an apoptosis trigger. Furthermore, the progressive deposition of extracellular matrix as seen in the cystic kidneys may eventually disrupt normal cell-matrix interactions of epithelia, which would provide a hostile environment for tubular cell survival that ultimately leads cells to die. Such disturbance of the microenvironment that surrounds the cysts could potentially function to elicit epithelial cell apoptosis.

Overall, we have established an improved animal model that mimics the human form of ADPKD. Notably, the renal cystic phenotype is caused by *Pkd1* knockdown rather than knockout. That is why our model can avoid the embryonic or prenatal lethality caused by *Pkd1* knockout. We do not know whether the *PKD1* down-regulation actually occurs in human ADPKD patients or whether it causes the renal cystic phenotype. However, the many similarities in disease progression and pathological findings between human ADPKD and homologous *Pkd1* knockdown mice suggest this $Pkd1^{L3/L3}$ mouse may serve as an attractive model to study pathogenesis and to explore novel therapeutic strategies against ADPKD.

## Acknowledgments

We thank Y.-L. Chien and L. Lu for assistant in generation of *Pkd1* targeted mutant mice.

## References

1. Torres VE, Harris PC: Autosomal dominant polycystic kidney disease. Nefrologia 2003, 23:14–22
2. Verani RR, Silva FG: Histogenesis of the renal cysts in adult (autosomal dominant) polycystic kidney disease. A histochemical study. Mod Pathol 1988, 1:457–463
3. Wilson PD: Polycystic kidney disease. N Engl J Med 2004, 350:151–164
4. European Polycystic Kidney Disease Consortium: The polycystic kidney disease 1 gene encodes a 14 kb transcript and lies within a duplicated region on chromosome 16. Cell 1994, 77:881–894
5. American Polycystic Kidney Disease Consortium: Analysis of the genomic sequence for the autosomal dominant polycystic kidney disease gene (PKD1) predicts the presence of a leucine-rich repeat. Hum Mol Genet 1995, 4:575–582
6. International Polycystic Kidney Disease Consortium: Polycystic kidney disease: the complete structure of the PKD1 gene its protein. Cell 1995, 81:289–298
7. Mochizuki T, Wu G, Hayashi T, Xenophontos XL, Veldhuisen B, Saris JJ, Reynolds DM, Cai Y, Gabow PA, Pierides A, Kimberling WJ, Breuning MH, Deltas CC, Peters DJM, Somlo S: PKD2, a gene for polycystic kidney disease that encodes an integral membrane protein. Science 1996, 272:1339–1342
8. Qian F, Watnick TJ, Onuchic LF, Germino GG: The molecular basis of focal cyst formation in human autosomal dominant polycystic kidney disease type I. Cell 1996, 87:979–987
9. Watnick TJ, He N, Wang K, Liang Y, Parfrey P, Hefferton D, St. George-Hyslop P, Germino G, Pei Y: Somatic mutations of PKD1 in ADPKD2 cystic tissue suggests a possible pathogenic effect of transheterozygous mutations. Nat Genet 2000, 25:143–144
10. Lu W, Peissel B, Babakhanlou H, Pavlova A, Geng L, Fan X, Larson C, Brent G, Zhou J: Perinatal lethality with kidney and pancreas defects in mice with a targeted Pkd1 mutation. Nat Genet 1997, 17:179–181
11. Lu W, Shen X, Pavlova A, Lakkis M, Ward CJ, Pritchard L, Harris PC, Genest DR, Perex-Atayde AR, Zhou J: Comparison of Pkd1-targeted mutants reveals that loss of polycystin-1 causes cystogenesis and bone defects. Hum Mol Genet 2001, 10:2385–2396
12. Wu G, D'Adati V, Cai Y, Markowitz G, Park JH, Reynolds DM, Maeda Y, Le TC, Hou H, Kucherlapati R, Edelmann W, Somlo S: Somatic inactivation of Pkd2 results in polycystic kidney disease. Cell 1998, 93:177–188
13. Brasier JL, Henske EP: Loss of the polycystic kidney disease (PKD1) region of chromosome 16p13 in renal cyst cells supports a loss-of-function model for cyst pathogenesis. J Clin Invest 1997, 99:194–199
14. Ong AC, Harris PC, Davies DR, Pritchard L, Rossetti S, Biddolph S, Vaux DJ, Migone N, Ward CJ: Polycystin-1 expression in PKD1, early-onset PKD1, and TSC2/PKD1 cystic tissue. Kidney Int 1999, 56:1324–1333
15. Delmas P, Nomura H, Li X, Lakkis M, Luo Y, Segal Y, Fernández-Fernández JM, Harris P, Frischauf A, Brown DA, Zhou J: Constitutive activation of G-proteins by polycystin-1 is antagonized by polycystin-2. J Biol Chem 2002, 277:11276–11283
16. Delmas P, Padilla F, Osorio N, Coste B, Raoux M, Crest M: Polycystins, calcium signaling, and human diseases. Biochem Biophys Res Commun 2004, 322:1374–1383
17. Wilson PD: Polycystin new aspects of structure, function, and regulation. J Am Soc Nephrol 2001, 12:834–845
18. Nauli SM, Alenghat FJ, Luo Y, Williams E, Vassilev P, Li X, Elia AEH, Lu W, Brown EM, Quinn SJ, Ingber DE, Zhou J: Polycystins 1 and 2 mediate mechanosensation in the primary cilium of kidney cells. Nat Genet 2003, 33:129–137
19. Ward CJ, Turley H, Ong AC, Comley M, Biddolph S, Chetty R, Ratcliffe PJ, Gattner K, Harris PC: Polycystin, the polycystic kidney disease 1 protein, is expressed by epithelial cells in fetal, adult, and polycystic kidney. Proc Natl Acad Sci USA 1996, 93:1524–1528
20. Geng L, Segal Y, Peissel B, Deng N, Pei Y, Carone F, Rennke HG,

Glucksmann-Kuis AM, Schneider MC, Ericsson M, Reeders ST, Zhou J: Identification and localization of polycystin, the PKD1 gene product. J Clin Invest 1996, 98:2674–2682
21. van Adelsberg J, Chamberlain S, D'Agati V: Polycystin expression is temporally and spatially regulated during renal development. Am J Physiol 1997, 272:F602–F609
22. Kim K, Drummond I, Ibraghimov-Beskrovnaya O, Klinger K, Arnaout A: Polycystin 1 is required for the structural integrity of blood vessels. Proc Natl Acad Sci USA 2000, 97:1731–1736
23. Boulter C, Mulroy S, Webb S, Fleming S, Brindle K, Sandford R: Cardiovascular, skeletal, and renal defects in mice with a targeted disruption of the Pkd1 gene. Proc Natl Acad Sci USA 2001, 98:12174–12179
24. Nadasdy T, Laszik Z, Lajoie G, Blick KE, Wheeler DE, Silva FG: Proliferative activity of cyst epithelium in human renal cystic diseases. J Am Soc Nephrol 1995, 5:1462–1468
25. Woo D: Apoptosis and loss of renal tissue in polycystic kidney diseases. N Engl J Med 1995, 333:18–25
26. Wilson PD, Du J, Norman JT: Autocrine, endocrine and paracrine regulation of growth abnormalities in autosomal dominant polycystic kidney disease. Eur J Cell Biol 1993, 61:131–138
27. Sakai M, Zhang MZ, Homma T, Garrick B, Abraham JA, McKanna JA, Harris RC: Production of heparin binding epidermal growth factor-like growth factor in the early phase of regeneration after acute renal injury. J Clin Invest 1997, 99:2128–2138
28. Dell KM, Nemo R, Sweeney WE, Avner ED: EGF-related growth factors in the pathogenesis of murine ARPKD. Kidney Int 2004, 65:2018–2029
29. Wetzel RK, Sweadner KJ: Immunocytochemical localization of Na-K-ATPase $\alpha$- and $\beta$-subunits in rat kidney. Am J Physiol 2001, 281:F531–F545
30. Torres VE, Wang X, Qian Q, Somlo S, Harris PC, Gattone VH: Effective treatment of an orthologous model of autosomal dominant polycystic kidney disease. Nat Med 2004, 10:363–364
31. Geng L, Segal Y, Pavlova A, Barros EJ, Lohning C, Lu W, Nigam SK, Frischauf AM, Reeders ST, Zhou J: Distribution and developmentally regulated expression of murine polycystin. Am J Physiol 1997, 272:F451–F459
32. Waldherr R, Zerres K, Gall A, Enders H: Polycystic kidney disease in the fetus. Lancet 1989, 2:274–275
33. Michaud J, Russo P, Grignon A, Dallaire L, Bichet D, Rosenblatt E, Lamothe E, Lambert M: Autosomal dominant polycystic kidney disease in the fetus. Am J Med Genet 1994, 51:240–246
34. Foggensteiner L, Bevan AP, Thomas R, Coleman N, Boulter C, Bradley J, Ibraghimov-Beskrovnaya O, Klinger K, Sandford R: Cellular and subcellular distribution of polycystin-2, the protein product of the PKD2 gene. J Am Soc Nephrol 2000, 11:814–827
35. Milutinovic J, Rust PF, Fialkow PJ, Agodoa LY, Phillips LA, Rudd TG, Sutherland S: Intrafamilial phenotypic expression of autosomal dominant polycystic kidney disease. Am J Kidney Dis 1992, 19:465–472
36. Koptides M, Mean R, Demetriou K, Pierides A, Deltas CC: Genetic evidence for a trans-heterozygous model for cystogenesis in autosomal dominant polycystic kidney disease. Hum Mol Genet 2000, 9:447–452
37. Wu G, Tian X, Nishimura S, Markowitz GS, D'Agati V, Park JH, Yao L, Li L, Geng L, Zhao H, Edelmann W, Somlo S: Trans-heterozygous Pkd1 and Pkd2 mutations modify expression of polycystic kidney disease. Hum Mol Genet 2002, 11:1845–1854
38. Cook DL, Gerber AN, Tapscott SJ: Modeling stochastic gene expression: implications for haploinsufficiency. Proc Natl Acad Sci USA 1998, 95:15641–15646
39. Yoder BK, Hou X, Guay-Woodford LM: The polycystic kidney disease proteins, polycystin-1, polcystin-1, polaris and cystin are co-localized in renal cilia. J Am Soc Nephrol 2002, 13:2508–2516
40. Huan Y, van Adelsberg J: Polycystin-1, the PKD1 gene product, is in a complex containing E-cadherin and the catenins. J Clin Invest 1999, 104:1459–1468
41. Scheffers MS, van der Bent P, Prins F, Spruit L, Breuning MH, Litvinov SV, de Heer E, Peters DJ: Polycystin-1, the product of the polycystic kidney disease 1 gene, co-localizes with desmosomes in MDCK cells. Hum Mol Genet 2000, 9:2743–2750
42. Geng L, Burrow CR, Li HP, Wilson PD: Modification of the composition of polycystin-1 multiprotein complexes by calcium and tyrosine phosphorylation. Biochim Biophys Acta 2000, 1535:21–35
43. Roitbak T, Ward CJ, Harris PC, Bacallao R, Ness SA, Wandinger-Ness A: A polycystin-1 multiprotein complex is disrupted in polycystic kidney disease cells. Mol Biol Cell 2004, 15:1334–1346
44. Du J, Wilson PD: Abnormal polarization of EGF receptors and autocrine stimulation of cyst epithelial growth in human ADPKD. Am J Physiol 1995, 269:C487–C495
45. Wilson PD, Devuyst O, Li X, Gatti L, Falkenstein D, Robinson S, Fambrough D, Burrow CR: Apical plasma membrane mispolarization of Na-K-ATPase in polycystic kidney disease epithelia is associated with aberrant expression of the $\beta_2$ isoform. Am J Pathol 2000, 156:253–268
46. Ogborn MR, Sareen S, Tomobe K, Takahashi H, Crocker JF: Renal tubule Na-K-ATPase polarity in different animal models of polycystic kidney disease. J Histochem Cytochem 1995, 43:785–790
47. Brill SR, Ross KE, Davidow CJ, Ye M, Grantham JJ, Caplan MJ: Immunolocalization of ion transport proteins in human autosomal dominant polycystic kidney epithelial cells. Proc Natl Acad Sci USA 1996, 93:10206–10211
48. Jones EA, Shahed A, Shoskes DA: Modulation of apoptotic and inflammatory genes by bioflavonoids and angiotensin II inhibition in ureteral obstruction. Urology 2000, 56:346–351